



BNL-105239-2014-TECH

Booster Technical Note No. 195;BNL-105239-2014-IR

PROTON INJECTION INTO THE AGS BOOSTER (A MODEL STUDY IN THE HORIZONTAL PLANE)

M. Blaskiewicz

August 1991

Collider Accelerator Department
Brookhaven National Laboratory

U.S. Department of Energy

USDOE Office of Science (SC)

Notice: This technical note has been authored by employees of Brookhaven Science Associates, LLC under Contract No. DE-AC02-76CH00016 with the U.S. Department of Energy. The publisher by accepting the technical note for publication acknowledges that the United States Government retains a non-exclusive, paid-up, irrevocable, world-wide license to publish or reproduce the published form of this technical note, or allow others to do so, for United States Government purposes.

DISCLAIMER

This report was prepared as an account of work sponsored by an agency of the United States Government. Neither the United States Government nor any agency thereof, nor any of their employees, nor any of their contractors, subcontractors, or their employees, makes any warranty, express or implied, or assumes any legal liability or responsibility for the accuracy, completeness, or any third party's use or the results of such use of any information, apparatus, product, or process disclosed, or represents that its use would not infringe privately owned rights. Reference herein to any specific commercial product, process, or service by trade name, trademark, manufacturer, or otherwise, does not necessarily constitute or imply its endorsement, recommendation, or favoring by the United States Government or any agency thereof or its contractors or subcontractors. The views and opinions of authors expressed herein do not necessarily state or reflect those of the United States Government or any agency thereof.

PROTON INJECTION INTO THE AGS BOOSTER
(A MODEL STUDY IN THE HORIZONTAL PLANE)

BOOSTER TECHNICAL NOTE
NO. 195A

M. BLASKIEWICZ and A. LUCCIO

AUGUST 6, 1991

ALTERNATING GRADIENT SYNCHROTRON DEPARTMENT
BROOKHAVEN NATIONAL LABORATORY
UPTON, NEW YORK 11973

PROTON INJECTION INTO THE AGS BOOSTER - A MODEL STUDY IN THE HORIZONTAL PLANE.

M.Blaskiewicz, A.Luccio

1. Introduction

It is convenient to recall the main features of proton injection into the AGS Booster, described in detail in the Booster Design Manual¹.

200 MeV H^- are injected into the AGS Booster from the linac. The injection takes place in one of the booster bending magnets (DHC5). The H^- are converted to protons in a stripping foil located shortly downstream from DHC5 and captured on a stable orbit around the ring. About 100 linac pulses are injected, filling as many RF buckets, three in each turn. Since at injection the booster revolution period is of the order of 1.2 μ sec, the total injection time is of the order of 40 μ sec.

Two orbit bumps are used to achieve the matching between the injected beam and the stored beam and to make the stored beam fill up the booster acceptance and bypass the foil in subsequent turns: A DC bump, obtained with trim coils on three of the bending magnets (DHC4, DHC8, DHD1) and a fast bump using four horizontal kickers (KHC1, KHC3, KHC7, KHD1). At the beginning of the injection process both bumps are active and bring the equilibrium orbit in the ring to the same phase space location on the foil where the injected beam is directed. Then, the fast bump start to collapse and the center of the equilibrium acceptance phase space figure moves steadily towards its final position. Because of collective betatron oscillations, at each turn the injected beam returns to the foil in a different radial position, gradually filling the acceptance area.

Figure 1 shows the horizontal phase space acceptance. There, we are looking along the direction of the injection beam. The foil is located to the right, towards the center of the booster. The final equilibrium orbit is to the left of the center of the acceleration chamber. Figure 2 shows the injection geometry through DHC5 as seen from above. To allow for the H^- beam to enter the magnet, part of the side return yoke has been removed. The curvature

¹ AGS Booster Design Manual, Rev 1, October 1988, pp. 4-5 to 4-9

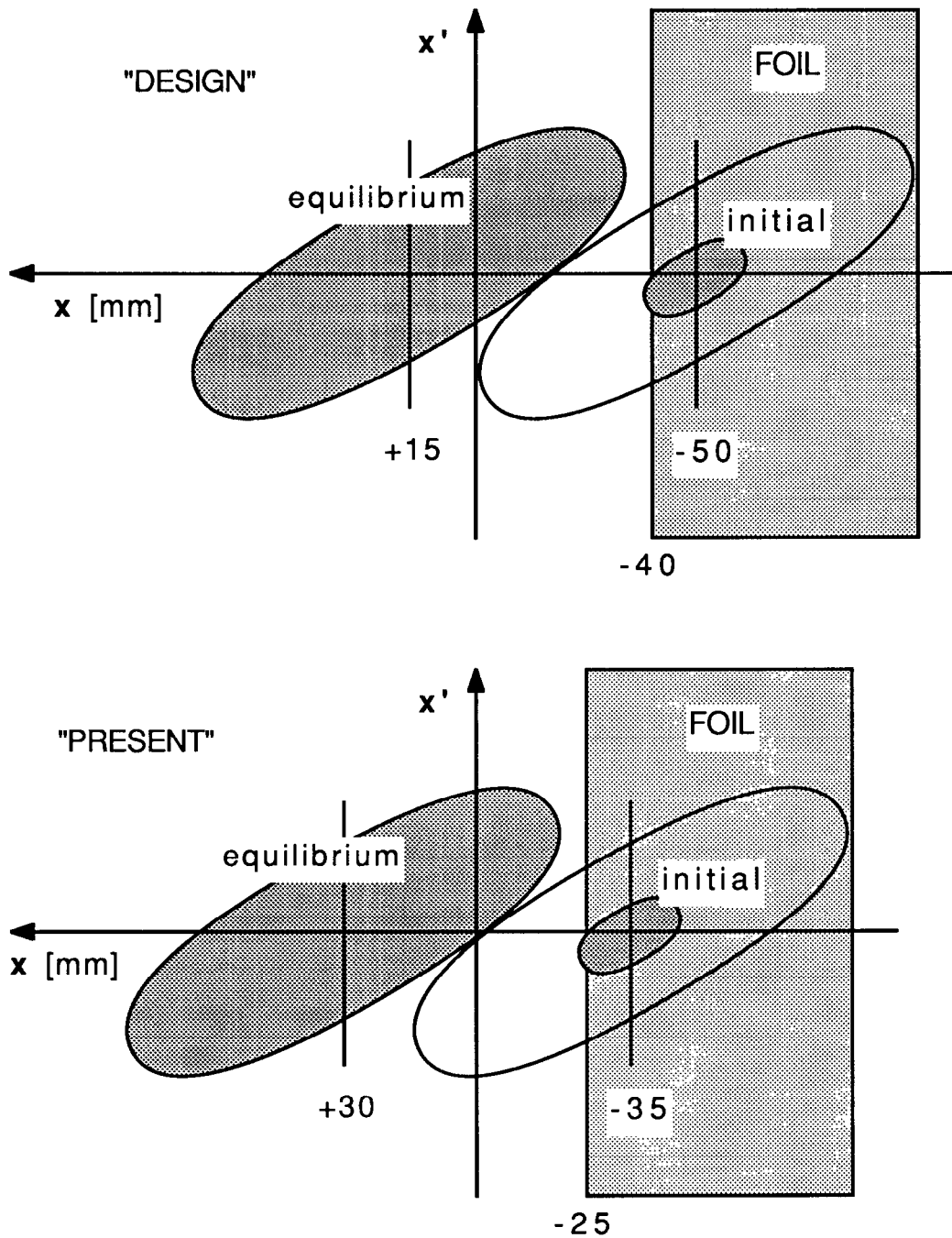


Fig.1. Schematic geometry of proton injection in the AGS Booster. The injected H^- beam travels into the page. The center of the Booster ring is located towards the right.

The large phase space ellipse represents the acceptance of the Booster, the small ellipse represents the first injected bunch. After the injection process is terminated, the filled acceptance is located at an equilibrium position to the left of the center of the acceleration chamber.

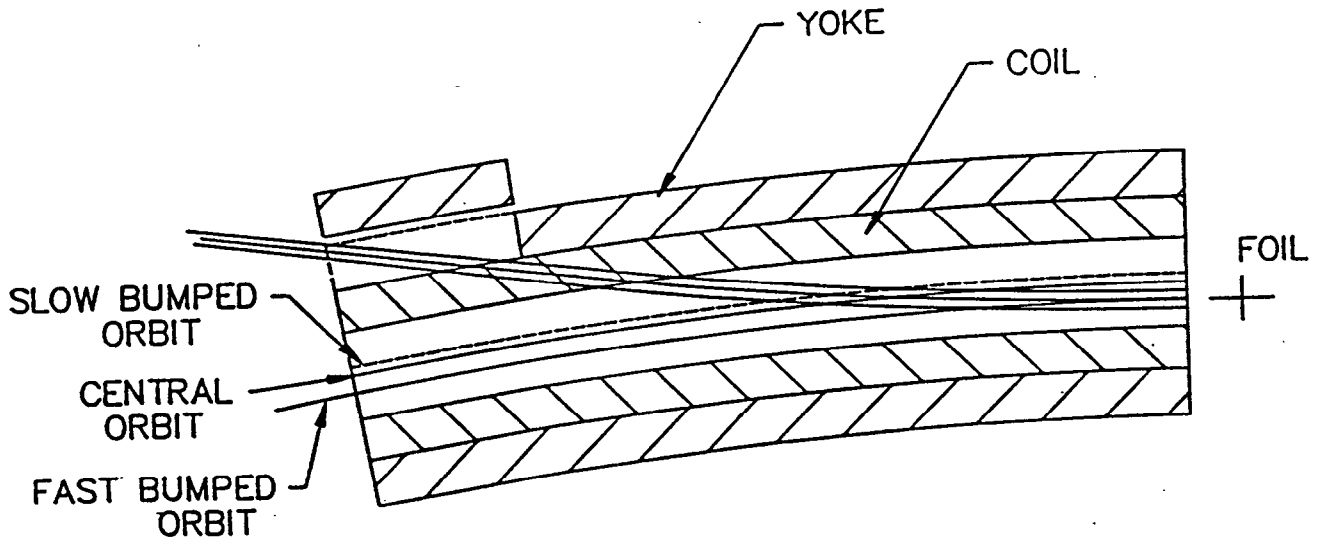


Fig.2. Proton injection through the DHC5 dipole.

of the negative beam orbit is opposite to the curvature of the protons obtained after stripping.

The model study of the injection process, in the limit of zero beam current, has been performed in three phases:

- 1 - Modeling of the DC and fast bumps acting on the circulating beam;
- 2 - Tracking of the injected beam through DHC5 and other optical elements;
- 3 - Study of the necessary steering in the LTB (Linac to Booster) line.

2. Bumps in the Booster

We studied bumps (DC plus fast) that would direct the circulating beam at the beginning of the injection through the foil at radial positions between -35 and -50 mm, with respect to the center of the vacuum chamber and at angles ranging from -10 to 10 mrad. The DC bump alone would bring the center of the beam from +30 to +15 mm respectively, therefore allowing for a 65 mm displacement, large enough to accommodate the booster aperture. Since the 90% diameter of the H^- is probably 20 mm at the foil (we used the

horizontal emittance $\epsilon_x = 8.32 \pi$ mm-mrad), the edge of the foil will be located between -25 and -40 mm in the above cases.

The "design" case is: injection at -50 mm, the "present" case is: injection at -35 mm. These two extreme cases are shown in Figure 1.

Figures 3, 4 and 5 show the effect of the bumps (DC + fast) on the circulating beam as calculated by MAD² for injection at -35, -40 and -45 mm, respectively. In each case the slow bump was calculated first, to bring the beam after injection at +65 mm away from the point of first injection as described earlier, then the 4-magnet fast bump was added. Using four magnets allows one also to choose the angle at the foil. We calculated bumps for obtaining 0, -2.5, -5, -7.5 and -10 mrad at the foil. The strength of the needed kicks³ for each case are given in Table 1.

The figures show that if one wants to limit the beam excursion to ± 70 mm, not all angles could be accepted.

3. Tracking through DHC5

MAD allows calculations around a reference trajectory. For the present geometry the reference trajectory can be calculated by direct integration of the equations of motion through the dipole field of DHC5, and other adjacent magnets. Ed Bleser already did this⁴ and here we simply repeated his calculations with greater accuracy, being aware that the results are very sensitive to small variations of the initial conditions and to the accuracy of the integration technique. With reference to Figure 6, in the plane (\mathbf{u}, \mathbf{v}) we integrate the equation

$$\frac{v''}{(1+v'^2)^{3/2}} = \frac{1}{\rho(u,v)} = \frac{eB(u,v)}{p}, \quad v' = \frac{dv}{du}$$

with the coordinate \mathbf{u} along the direction of injection (axis of LTB) and with \mathbf{p} particle's momentum. The prime denotes differentiation with respect to \mathbf{u} . The local values of the

² F.Ch.Iselin and J.Niederer. *The MAD Program, Version 7.02*, CERN/LEP-TH/88-38, Geneva July 13, 1988

³ A.Luccio. *Bumps in the AGS Booster*, Booster Technical Note No. 189, March 11, 1991

⁴ Ed Bleser, private communication

magnetic field are interpolated from values calculated with POISSON⁵ and checked against measurements (excellent agreement). The integration routine is a 3-rd order predictor-corrector⁶. During the integration, the quantity $B\rho$ is monitored and remains constant within one part in 10^{-6} . In this calculation the exit edge of the magnet is "hard"; since the H-beam emerges from DHC5 at an angle close to 90° , we assume that the hard edge approximation is adequate.

Table 1
Proton Injection Bumps

DC bump kick [mrad]			final		fast bump kick [mrad]				initial at foil	
DHC4	DHC8	DHD1	x [mm]	x'[mr]	KHC1	KHC3	KHC7	KHD1	x [mm]	x'[mr]
					-4.10	-9.50	-5.38	-6.35		0.
					-0.43	-9.41	-1.53	-8.12		-2.5
-3.84	-0.36	-4.19	30	6.24	3.23	-9.32	2.34	-9.89	-35	-5.0
					6.89	-9.23	6.19	-11.66		-7.5
					10.56	-9.14	10.1	-13.43		-10.
					-5.66	-9.57	-7.04	-5.62		0.
					-2.00	-9.48	-3.18	-7.39		-2.5
-3.20	-0.30	-3.48	25	5.20	1.66	-9.39	0.68	-9.16	-40	-5.0
					5.33	-9.30	4.54	-10.93		-7.5
					8.99	-9.20	8.40	-12.70		-10.
					-7.18	-9.60	-8.63	-4.88		0.
					-3.51	-9.51	-4.77	-6.65		-2.5
-2.56	-0.24	-2.79	20	4.16	0.15	-9.42	0.91	-8.42	-45	-5.0
					3.81	-9.32	2.95	-10.19		-7.5
					7.48	-9.23	6.81	-11.96		-10.
					-8.69	-9.27	-10.23	-4.14		0.
					-5.03	-9.54	-6.37	-5.91		-2.5
-1.92	-0.18	-2.09	15	3.12	-1.36	-9.45	-2.51	-7.68	-50	-5.0
					2.30	-9.36	1.35	-9.45		-7.5
					5.96	-9.26	5.21	-11.22		-10.

⁵ M.Goldman, private communication

⁶ HPCG, Hamming Predictor Corrector. A Library IBM Routine.

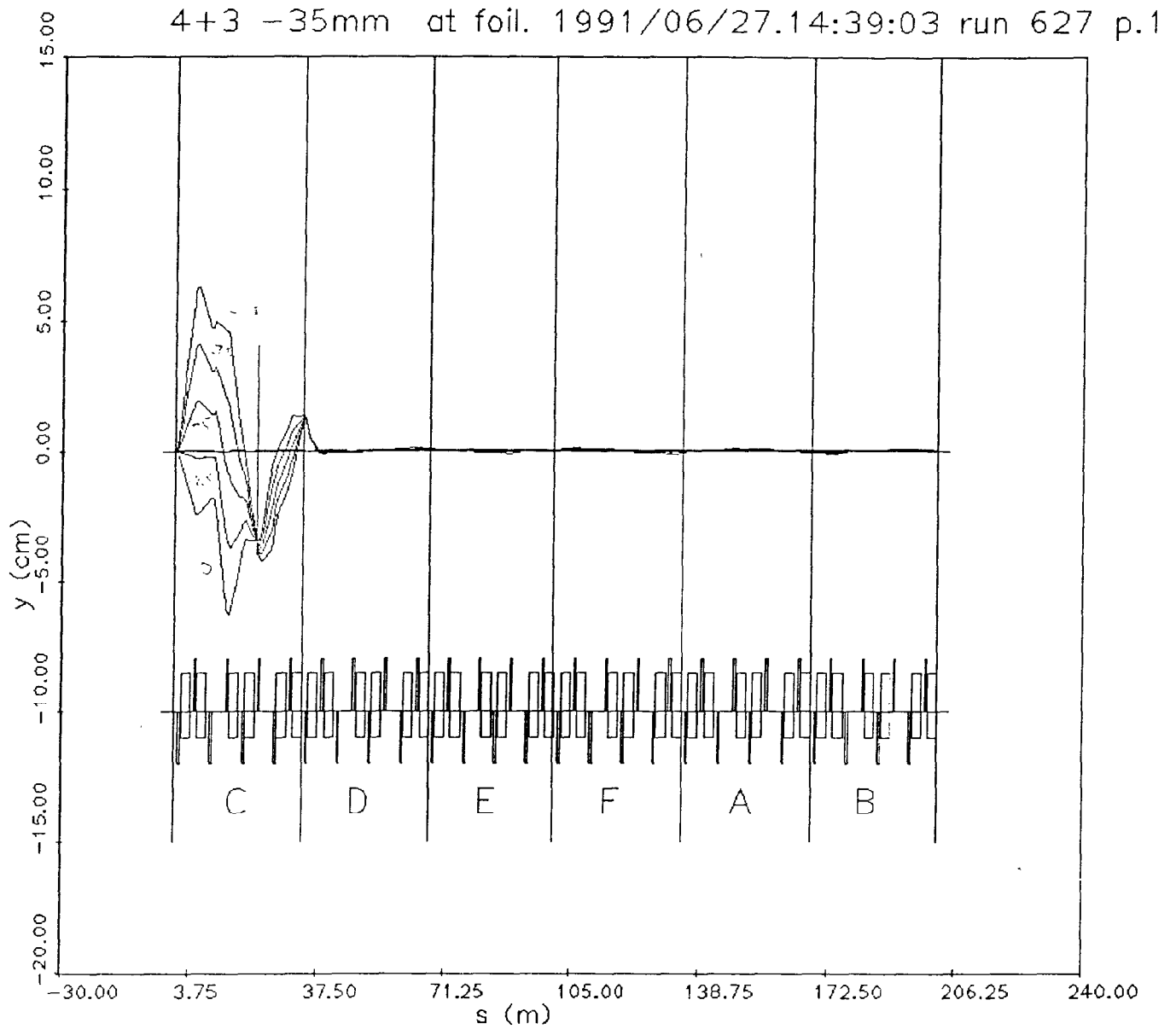


Fig.3. DC bump + fast bump (4 magnets) to locate the center of the beam at -35 mm at injection and +30 mm at equilibrium.

4+3 -40mm at foil. 1991/06/27.14:58:30 run 627 p.2

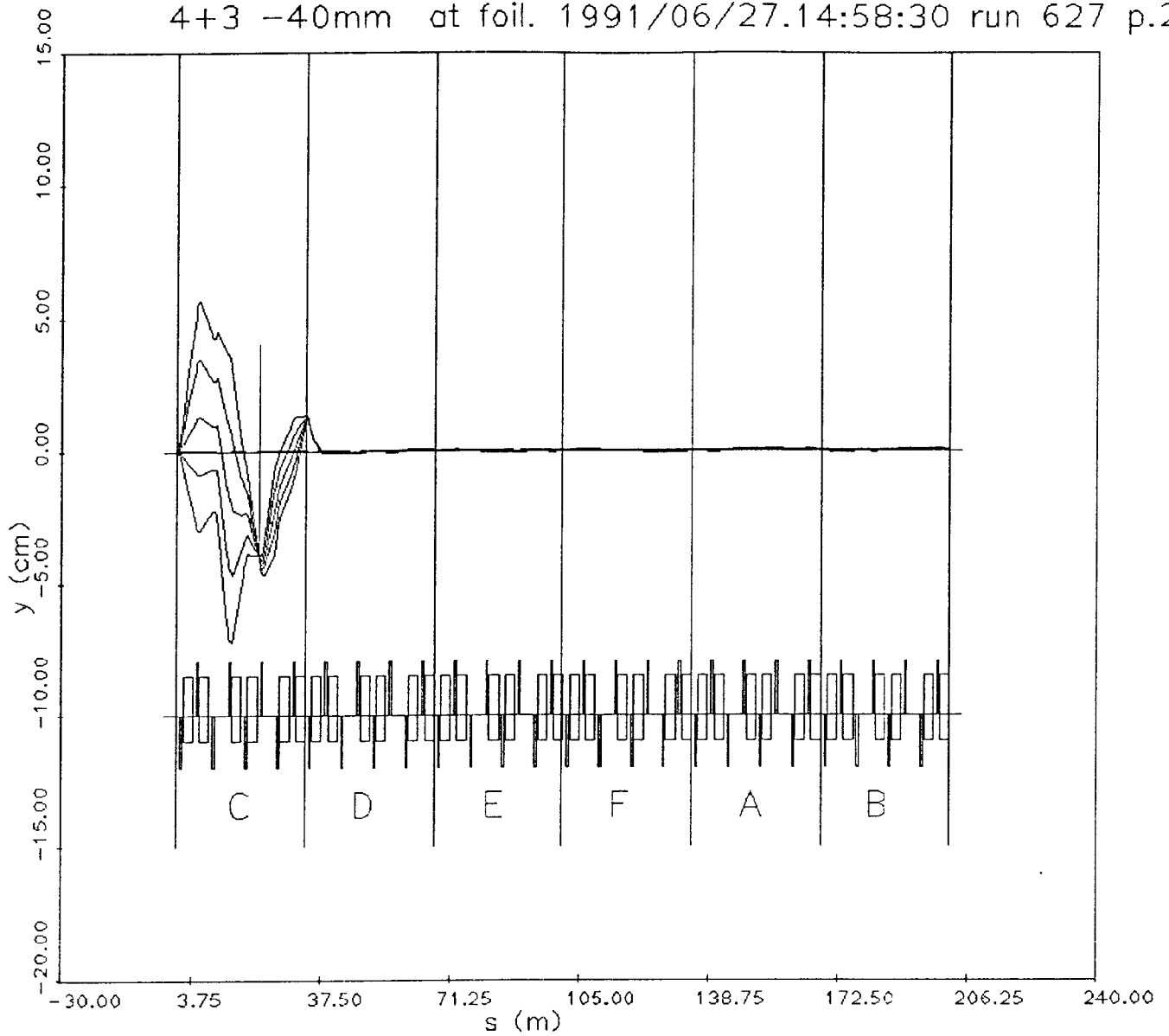


Fig.4. DC bump + fast bump (4 magnets) to locate the center of the beam at -40 mm at injection and +25 mm at equilibrium.

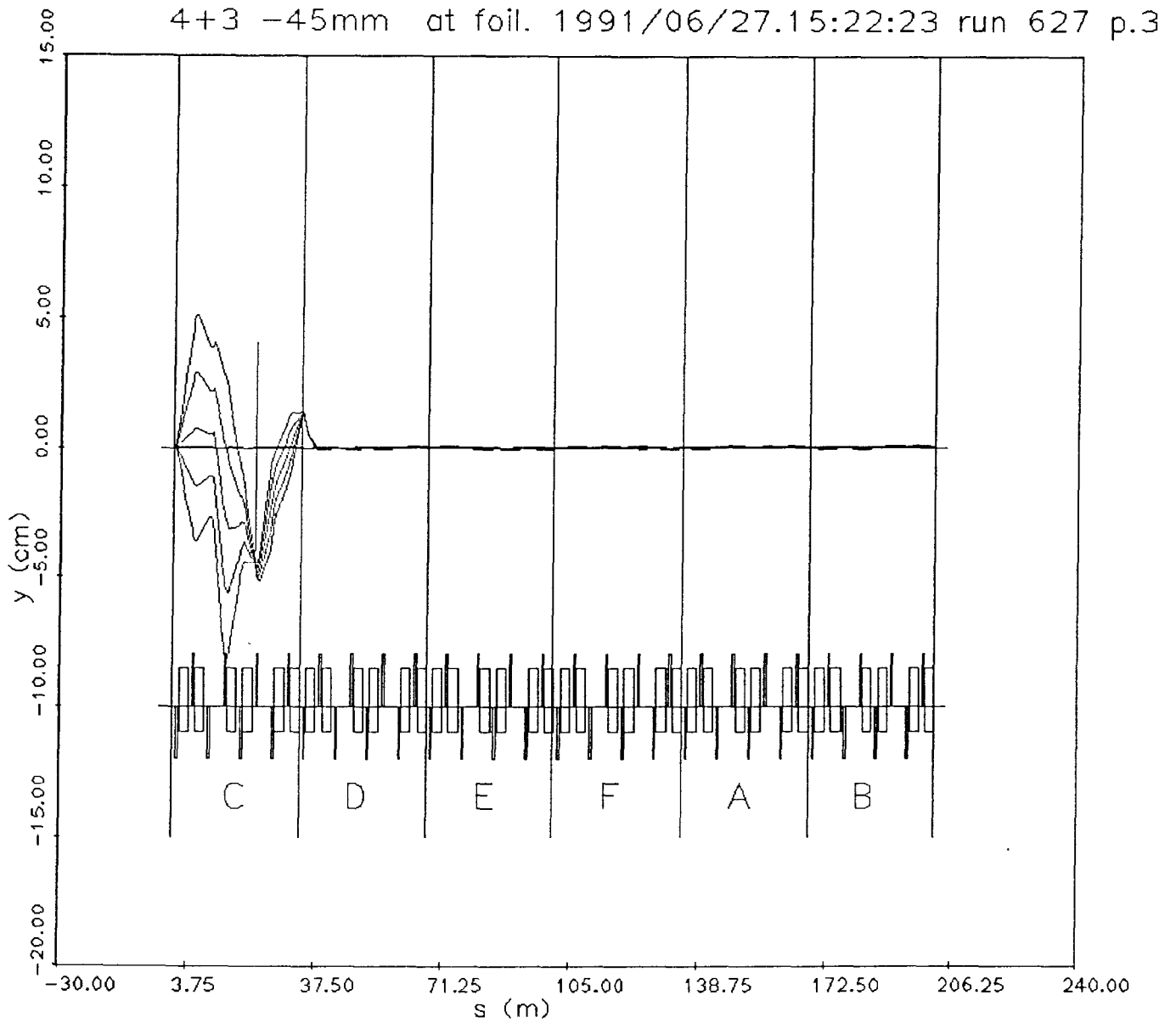


Fig.5. DC bump + fast bump (4 magnets) to locate the center of the beam at -45 mm at injection and +20 mm at equilibrium.

The geometry of the line, of the magnet and of the foil has been carefully checked against engineering drawings, survey and magnetic measurement data⁷. The key quantities, with reference to Figure 6, are the angle at the steel α' , the angle between the LTB line and the dipole chord θ and the distance between the center of the chord (steel), the intercept of the line axis with the chord $UB = d_o$ and the magnetic length of the arc $HE = l$. A constant datum is the magnetic angle of deflection $\alpha = 5^\circ$. The radius of curvature $\rho = l/\alpha$ is then calculated. The semi-width of the magnetic pole was taken as $w = 0.127$ m.

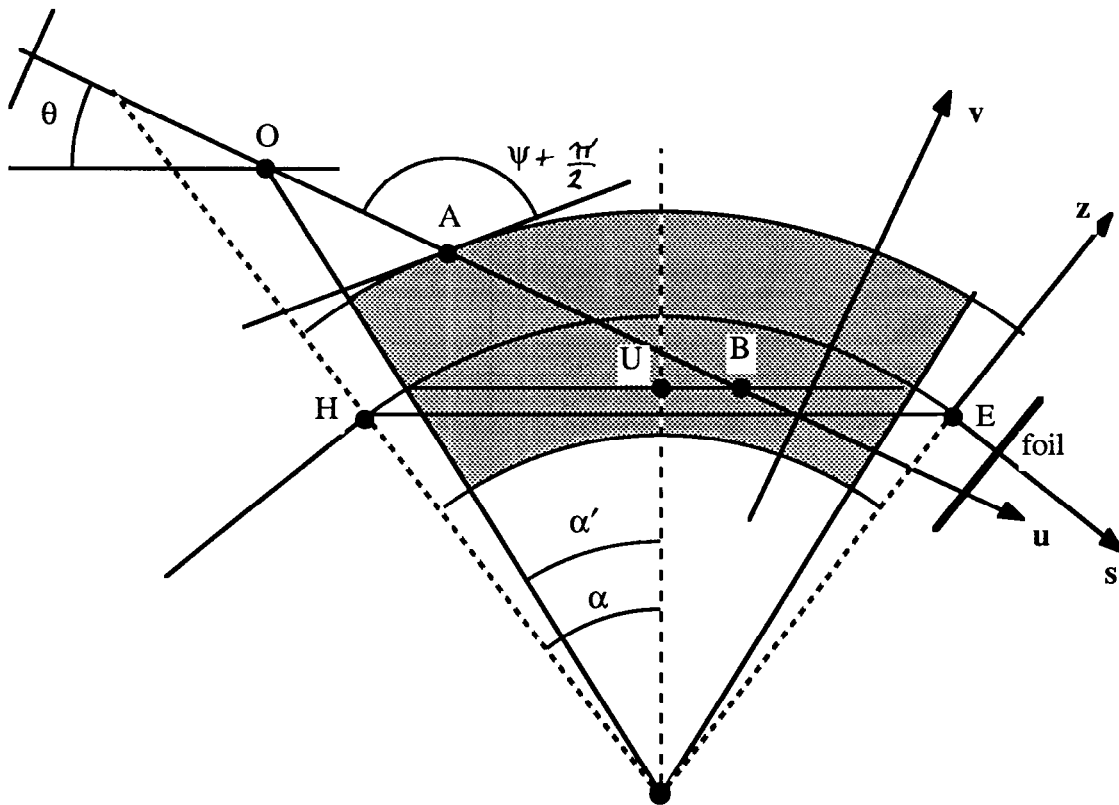


Fig.6. Geometry of the dipole DHC5 and of the injection line (u). The steel is shown as a shaded area. The boundaries of the physical magnet are also shown.

Figures 7, 8, and 9 show the result of the integration, forward, starting on the axis u at O and backwards, starting from -35 , -40 , and -45 mm at the foil, respectively. Each plot shows the trajectories corresponding to angles from 0 to -10 mrad at the foil. Resulting position and angle are given in Table 2 with reference to the coordinates of Figure 6.

⁷ R.Them, *Booster Dipole Production Measurements*, Booster Tech Note No. 190, March 13, 1991

It is

α'	4.99984°	(from survey, March 1991)
α	5°	by definition
θ	11° 58' 08"	(from survey, March 1991)
d_o	0.4478 m	(from survey, March 1991)
l	2.42 m	(from magnetic measurements)
$\rho = l/\alpha$	13.8657 m	

Table 2 (forward integration) shows that a beam sent along the axis reaches the foil close to the "design" position, and then that the original design of the line is correct. It also shows (backward) that the closer the foil is to the center line the larger the required displacement at the beginning of LTB.

From the integration, the length of the arc in the magnet and the magnetic field integral can be calculated. For the reference trajectory ($v, v' = 0$) the results are

$$\begin{aligned} \text{arc} &= 1.5974 \text{ m} \\ \int B \, dl &= 0.2583 \text{ tesla-m} \end{aligned}$$

Another important quantity is the angle ψ of entrance to the magnet at A, that determines the magnet's edge horizontal defocusing. It is

$$\psi = 1.335$$

-35 at foil. 1991/06/27.12:50:14 run 627 p.0

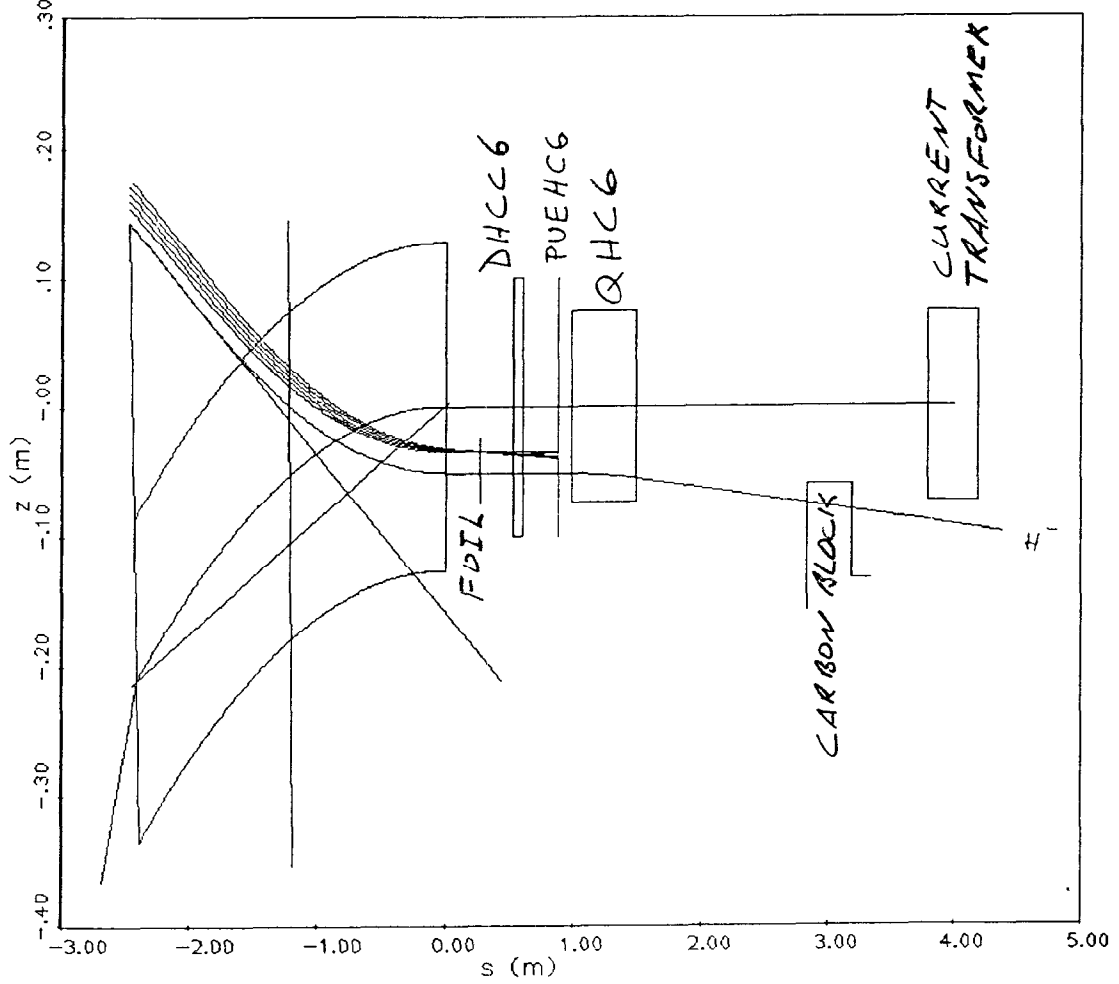


Fig.7. Integration through the dipole DHC5. Backward integration starting at -35 mm at the foil, with angles 0, -2.5, -5, -7.5 and -10 mrad.

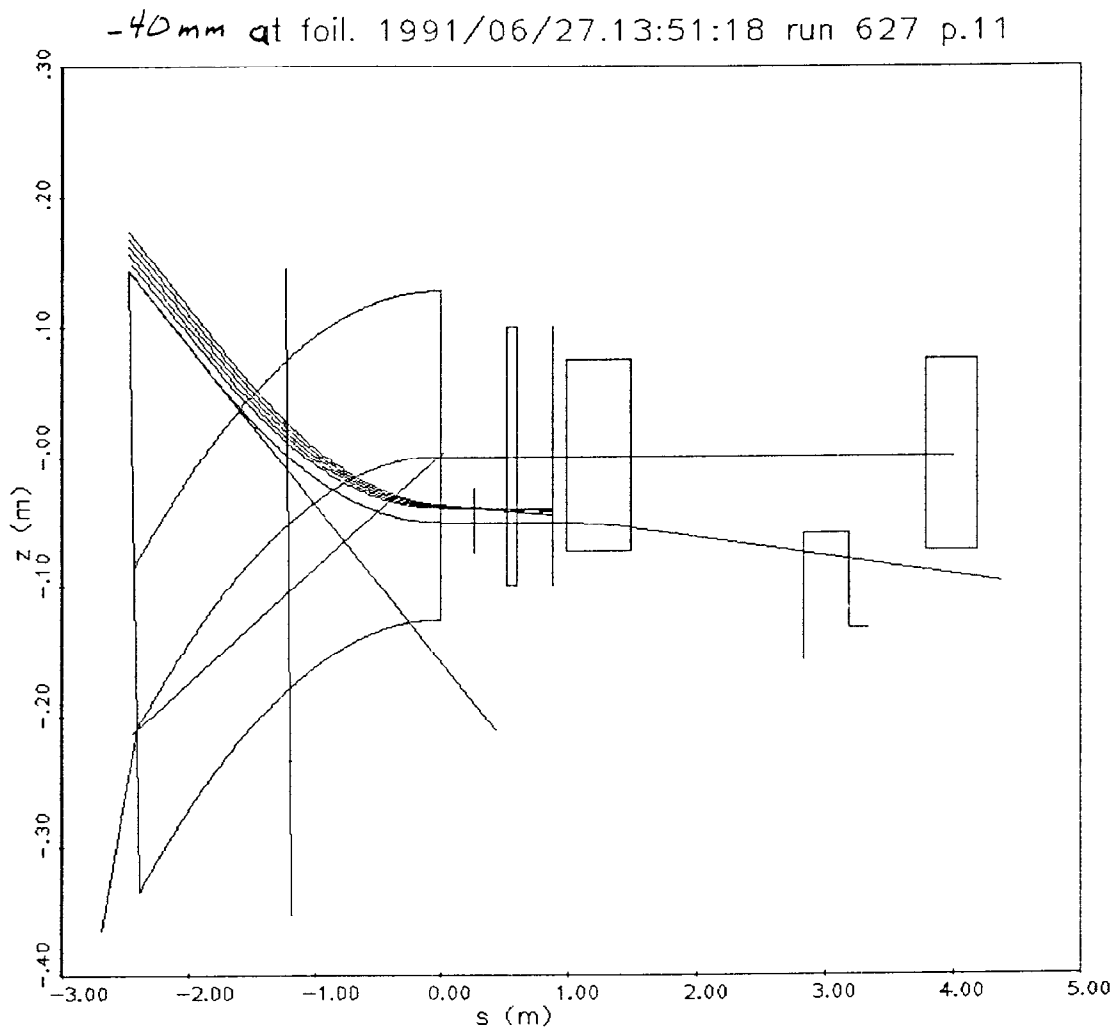


Fig.8. Integration through the dipole DHC5. Backward integration starting at -40 mm at the foil, with angles 0, -2.5, -5, -7.5 and -10 mrad.

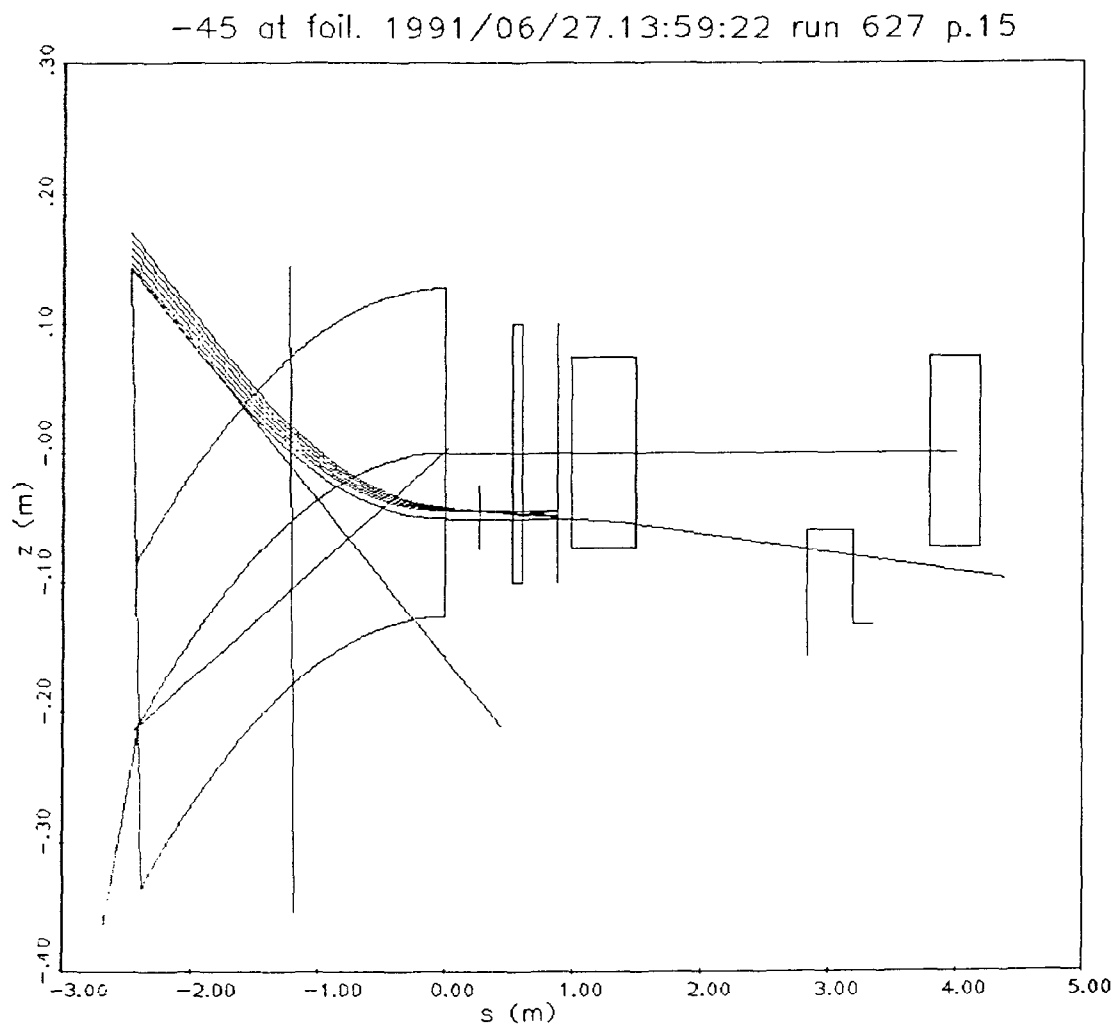


Fig.9. Integration through the dipole DHC5. Backward integration starting at -45 mm at the foil, with angles 0, -2.5, -5, -7.5 and -10 mrad.

Table 2
Integration through DHC5

Forward integration

LTB end (O)		foil	
v [mm]	v' [mrad]	z [mm]	z' [mrad]
0.	0.	-51.40	-0.87

Backward integration

foil		LTB end (O)		Figure
z [mm]	z' [mrad]	v [mm]	v' [mrad]	
	0.	10.73	5.01	
	-2.5	16.46	3.92	
-35	-5.0	22.18	2.81	7
	-7.5	27.87	1.69	
	-10.	33.56	0.56	
	0.	6.91	3.56	
	-2.5	12.67	2.47	
-40	-5.0	18.42	1.36	8
	-7.5	24.14	0.24	
	-10.	29.85	-0.9	
	0.	3.04	2.13	
	-2.5	8.83	1.04	
-45	-5.0	14.61	-0.08	9
	-7.5	20.37	-1.20	
	-10.	26.11	-2.33	

4. LTB modeling

Once the reference trajectory has been determined by direct integration, MAD can be used to model the LTB line down to the foil, in order to determine the modes of steering to achieve the necessary beam displacement and angle at O. This point, surveyed as the intercept of the LTB axis with a line extending from the entrance steel edge of DHC5 (see

Figure 6), is actually identified as a monitor MIOOO in MAD. The physical length of the magnet in MAD and the entrance angle to the magnet are arc and ψ calculated above. The exit angle is the reference angle at the foil given in Table 2. Finally, the angle of bend is given by arc/ρ .

MAD input for LTB	
ANGLE	-0.1155
E1	1.335
E2	-0.0078
L	1.5974

The first step for consistency check was to compare the transfer matrix between points MIOOO and FOIL in MAD, calculated from the twiss functions

$$\begin{pmatrix} \sqrt{\frac{\beta_2}{\beta_1}} (\cos \Delta\phi + \alpha_1 \sin \Delta\phi) & \sqrt{\beta_2 \beta_1} \sin \Delta\phi \\ -\frac{1}{\sqrt{\beta_2 \beta_1}} [(\alpha_2 - \alpha_1) \cos \Delta\phi + (1 + \alpha_2 \alpha_1) \sin \Delta\phi] & \sqrt{\frac{\beta_1}{\beta_2}} (\cos \Delta\phi - \alpha_1 \sin \Delta\phi) \end{pmatrix}$$

$$\Delta\phi = \phi_2 - \phi_1$$

and the horizontal transfer matrix obtained from the values of x, x' given in Table 2. The two matrices are shown below. We consider them in good agreement, showing in particular that the calculation of the edge focusing is reliable.

Integration	MAD
$M_x = \begin{pmatrix} 0.4399 & 2.313 \\ -.2890 & .7743 \end{pmatrix}$	$\begin{pmatrix} 0.4228 & 2.240 \\ -.3099 & .7232 \end{pmatrix}$

Horizontal steering in the last part of LTB, after the "big bend", can be accomplished with three magnets DH076, DH088 and DH112. The latter was indeed a vertical steering magnet that has been temporarily rotated by 90° and that presumably will be rotated back to serve its function in vertical painting. Using transfer matrices, it is found that the effect of the three magnets on the beam horizontal coordinates at MIOOO can be expressed as

$$x = .1745 \theta_{76} + 3.809 \theta_{88} + 4.031 \theta_{112}$$

$$x' = -.2700 \theta_{76} + .6298 \theta_{88} + \theta_{112}$$

LTB steer. 1991/07/11.10:09:50 run 708 p.1

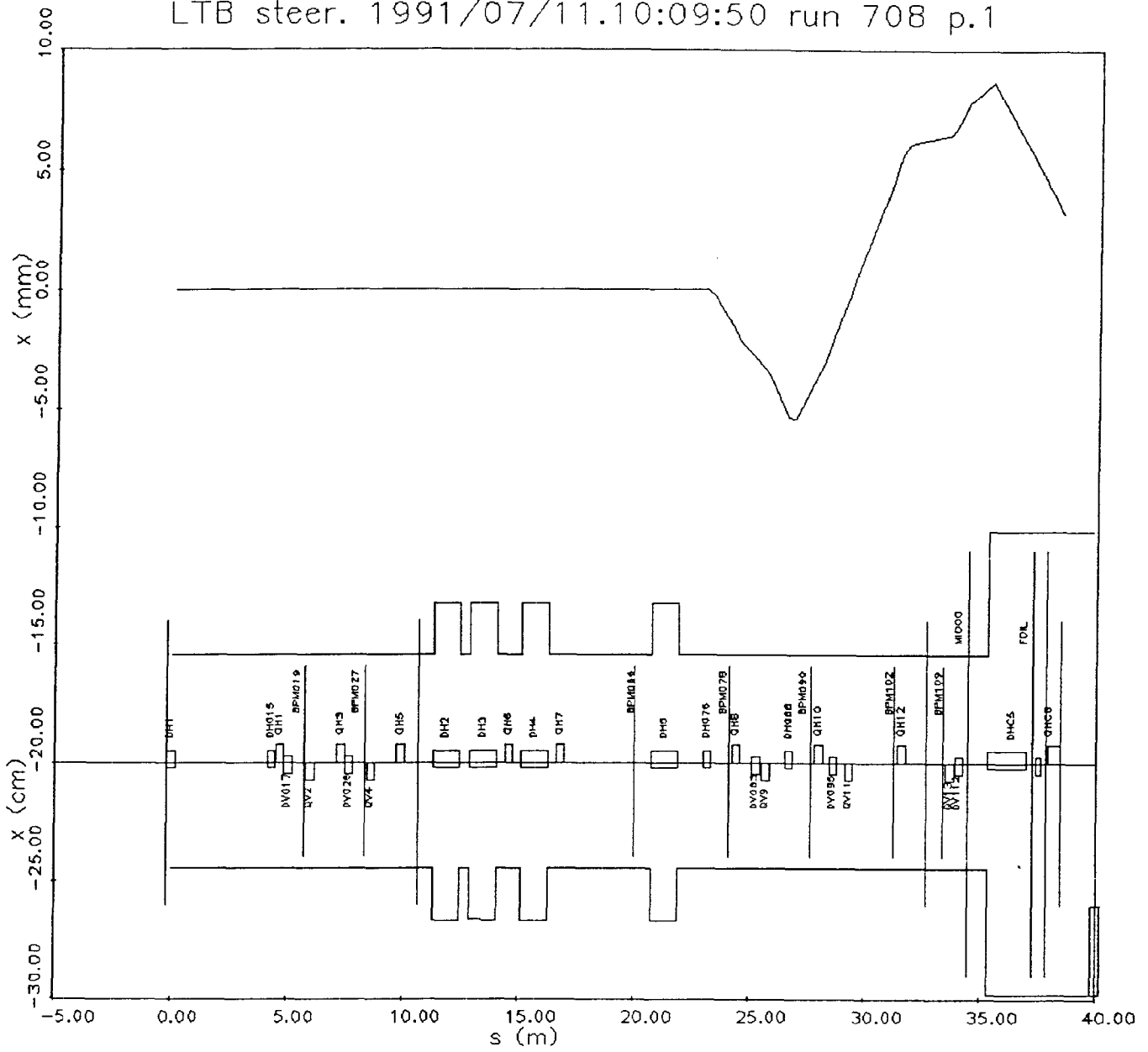


Fig.10. LTB trajectory to obtain 8.83 mm and 1.04 mrad at MIOOO.

Accordingly, and with no attempt to optimize, we find that a good solution to match at MIOOO e.g. the position and angles (8.83 mm, 1.04 mrad) for the case marked by the double edge boxes in Tables 1 and 2 can be achieved with the following kicks [mrad]

θ_{76}	θ_{88}	θ_{112}
-1.68	4.05	-2.00

The trajectory in the LTB line is shown in Figure 10. For this solution, we found in particular that the off-axis displacements at the quadrupoles following DH076 are the following [mm], which are no larger than the beam diameter

QH8	QV9	QH10	QV11	QH12	QV13
-2.267	-3.821	-3.031	0.356	6.071	6.864

5. Edge focusing

As shown in the expression for M_x , the entrance trajectory into the booster shows a net focusing in the horizontal plane. The transfer matrix for the vertical plane is

$$M_y = \begin{pmatrix} 1.628 & 3.301 \\ .3361 & 1.296 \end{pmatrix}$$

which has a net defocusing. As expected, the entrance edge of DHC5 acts as an horizontal quadrupole.

6. Conclusions

The paper machine results show that if the foil is located in a position close to the original design, the injection can be accomplished within the present capability of the available steering elements and that the present design of the injection geometry is basically correct. However, it is important to point out that recent measurements and beam injection studies (E.Bleser) show that the booster reality is difficult to understand and that before drawing any firm conclusion a careful comparison between experimental and model results is in order.

PROTON INJECTION INTO THE AGS BOOSTER - A MODEL STUDY IN THE HORIZONTAL PLANE.

Addendum

M.Blaskiewicz, A.Luccio

Limitations on booster aperture and bump magnet strengths place severe limitations on the possible configurations for proton injection in the Booster. Namely, the DC bump power supplies limit the equilibrium displacement of the circulating beam to no more than 25 mm; the fast kicker capabilities (7.5 mrad) limit the radial motion of the beam between initial injection and equilibrium to no more than 50 mm; and finally the booster aperture puts limits on the beam position at the foil at injection.

We assumed ± 40 mm as a radial width of the booster acceptance. This value is probably somewhat larger than the radial half width that can be injected to the AGS (assumed to be 1.3" or 33 mm), so our estimates have a safety factor. Since the aperture at the foil is ± 3 " (76.2 mm), to accommodate a 40 mm acceptance, we must inject at -35 mm. From measurements in the LTB and calculations of the Twiss functions for the line, the 65 % (one- σ) horizontal emittance translates into a beam ± 9 mm wide at the foil. Then, a good position of the foil is with its edge at -25 mm from the center of the aperture.

For the three DC bump only the offset (15 mm) can be prescribed. The resulting angle of the circulating beam is 3 mrad at the foil. A 4 kicker fast bump allows one to choose both position and angle at the foil. The position will be -35 mm. We choose the angle that minimizes the kicker strength and at the same time does not produce a wide beam excursion in other parts of the ring within the bump, particularly at the quadrupole QH4. An angle of -5 mrad at the foil appears a good choice as shown in Figure 1A. The effect of the DC bump alone is also shown.

The phase space relevant to the proposed injection process is shown in Figure 2A. The kicks required for this configuration are given in the table.

4+3, (-35,-5) at foil. 1991/07/19.14:06:17 run 719 p.2

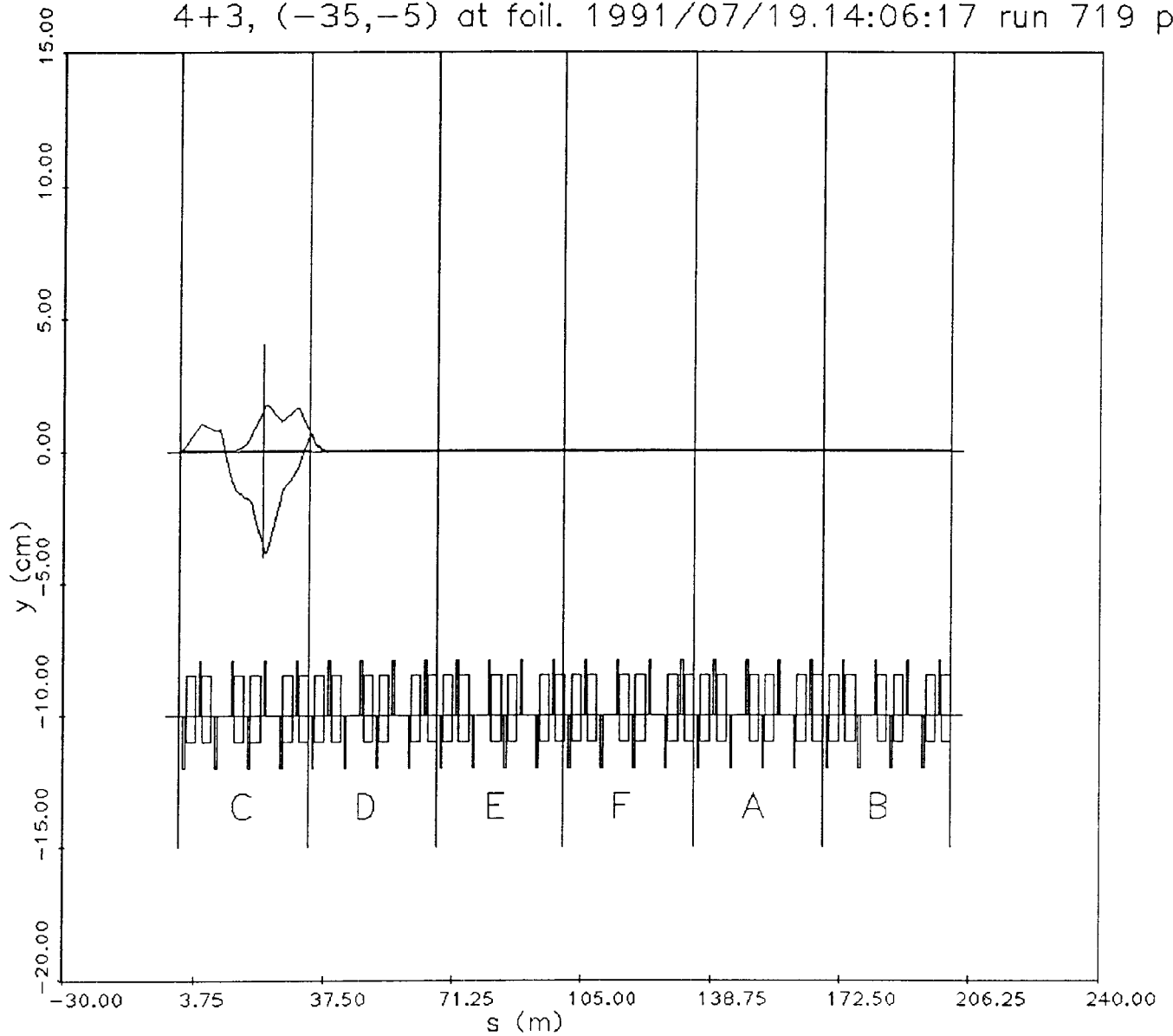


Fig. 1A. Equilibrium orbit for circulating beam (DC bump: +15 mm, +3 mrad) and beam during initial injection (DC bump + fast bump: -35 mm, -5 mrad) at foil.

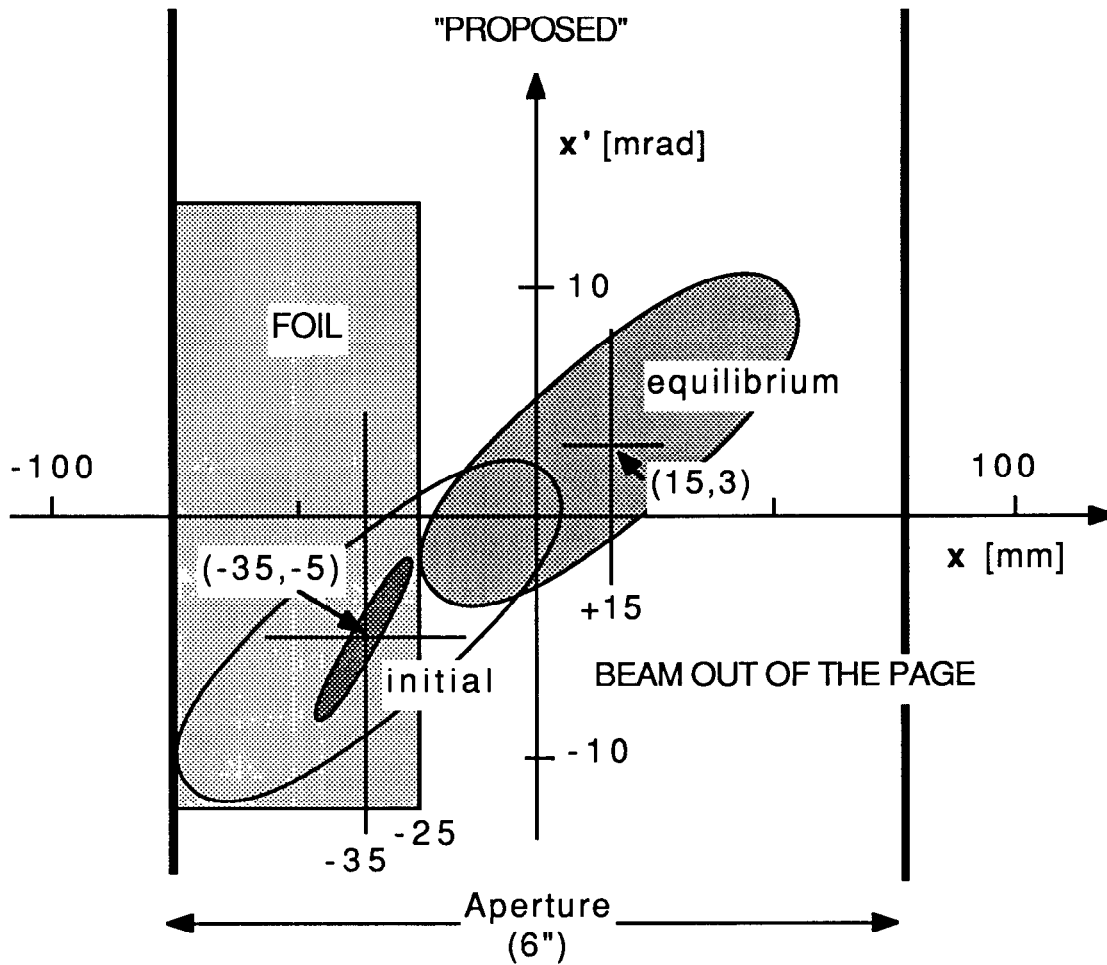


Fig. 2A. Phase space at initial injection and for circulating beam. Opposite convention than for Figure 1: the center of the Booster is on the left; the beam comes out of the page.

Fast injection bump [mrad], to displace beam by 50 mm, from +15 to -35 mm:

KHC1	KHC3	KHC7	KHD1
1.7	-7.2	0.99	-7.2

Slow TDH bump [mrad], to displace beam to +15 mm, 3.12 mrad:

DHC4	DHC8	DHD1
-1.92	-0.18	-2.09

Given the current survey data, the resulting beam coordinates at the end of LTB are: (22.18 mm, 2.81 mrad). These values can be obtained by pivoting the LTB at DH5 (the last bending magnet in the line). Since this section is 12 meters long, and the required displacement is 22 mm, the line rotation gives 1.86 mrad of natural steering. Thus, the additional 0.95 mrad has to come from steering magnets in the line